Journal of the European Ceramic Society **9** (1992) 107–119

Reactions Within Quartz–Carbon Mixtures in a Nitrogen Atmosphere

M. Ekelund & B. Forslund

Department of Inorganic Chemistry, Arrhenius Laboratory, University of Stockholm, S-106 91 Stockholm, Sweden

(Received 15 January 1991; revised version received 5 July 1991; accepted 22 July 1991)

Abstract

A number of carbon–quartz mixtures have been heat-treated in nitrogen at different pressures. The experiments were performed in a gas autoclave (pressure = 0·1–6 MPa, temperature = 1400–1680°C) allowing nitrogen to flow through the sample holder at a controlled rate, with continuous measurement of carbon monoxide in the exhaust gas. The samples were characterised by electron microscopy and elemental analyses, X-ray diffraction techniques and differential scanning calorimetry.

The degree of conversion to Si_3N_4 in mixtures of different types was determined and compared with the amount of quartz consumed. It was found that by rapid heating (20°C/min) to high temperatures (1550, 1680°C) even a fairly coarse-grained SiO_2-reagent ($1\,m^2/g$) is rapidly transformed to amorphous SiO_2, with just a minor part converted to Si_3N_4. The nitridation process during this initial stage, and the subsequent continuous heating, is governed by temperature, total pressure, nitrogen flow rate and SiO_2 and C surface areas. The relative importance of these parameters for the Si_3N_4 yield is discussed. Nitridation was virtually complete after 1 h annealing of a mixture with a SiO_2 surface area of $1\,m^2/g$ at a high nitrogen flow $\simeq$ 20 litres/min. The SiO evaporation was found to be rate controlling under these conditions.

Eine Reihe von Kohlenstoff/SiO_2–Mischungen wurde bei verschiedenen Drücken in einer Stickstoffatmosphäre erhitzt. Die Experimente wurden in einem Gas–Autoklaven im Temperaturbereich von 1400°C bis 1600°C bei einem Druck von 0·1 MPa bis 6 MPa durchgeführt. Der Stickstoffdurchfluß durch den Probenhalter wurde kontrolliert. CO in der Abluft wurde kontinuierlich gemessen. Die Proben wurden mittels Elektronenmikroskopie, Röntgenbeugung sowie kalorimetrisch und auf ihre elementare Zusammensetzung hin untersucht. Der Grad der Unwandlung zu Si_3N_4 in den einzelnen Mischungen wurde bestimmt und mit dem Anteil verbrauchten SiO_2 verglichen. Es hat sich gezeigt, daß bei schnellem Aufheizen (20°C/min) auf hohe Temperaturen (1550, 1680°C) selbst relativ grobes SiO_2 ($1\,m^2/g$) rasch amorphes SiO_2 mit nur geringen Anteilen an Si_3N_4 bildet. Die Nitridierung wird in der Anfangsphase und bei weiterer Temperaturerhöhung hauptsächlich durch die Temperatur, den Druck, die N_2-Durchflußrate und die spezifische Oberfläche der SiO_2- und C-Ausgangsmaterialien beinflußt. Auf den Einfluß dieser Parameter auf die Si_3N_4-Bildung wird eingegangen. Für eine Mischung aus SiO_2 mit einer spezifischen Oberfläche von $1\,m^2/g$ und einem N_2-Durchfluß von ca. 20 l/min war die Nitridierung nach einer Stunde nahezu abgeschlossen. Unter diesen Bedingungen war die SiO-Verdampfung geschwindigkeitsbestimmend.

Un certain nombre de mélanges, carbone–quartz, ont subi un traitement thermique sous azote à différentes pressions. Les expériences ont été réalisées dans un autoclave à gaz (pression = 0·1–6 MPa et température = 1400–1680°C) permettant à l'azote de circuler à travers le support de l'échantillon à vitesse contrôlée, le taux de CO étant mesuré dans le gaz de sortie. Les échantillons ont été caractérisés par microscopie électronique et analyses élémentaires, diffraction X et calorimétrie à balayage différentiel. Le taux de conversion en Si_3N_4 dans différents mélanges a été déterminé et comparé à la quantité de quartz consommée. Nous avons déterminé que, par chauffe rapide (20°C/min) jusqu'à haute température (1550, 1680°C), même un réactif SiO_2 à gros grain ($1\,m^2/g$) est rapidement transformé en SiO_2

Journal of the European Ceramic Society 0955-2219/92/$5.00 © 1992 Elsevier Science Publishers Ltd, England. Printed in Great Britain

amorphe, une part mineure étant transformée en Si_3N_4. Le processus de nitruration, pendant cette phase initiale et pendant la chauffe continue qui suit, est gouverné par la température, la pression totale, le débit d'azote et les surfaces spécifiques de SiO_2 et C. L'importance relative de ces paramètres quant à la formation de Si_3N_4 est discutée. En utilisant du SiO_2 de surface spécifique 1 m^2/g sous un flux d'azote élévé de 20 l/min, la nitruration du mélange est virtuellement complète après une heure de recuit. On montre que, dans ces conditions, l'évaporation de SiO contrôle la vitesse.

1 Introduction

The preparation of Si_3N_4 by carbothermic reduction and simultaneous nitridation of SiO_2 has been studied for almost a century. Despite these efforts we still have insufficient knowledge of how to optimise the process so as to produce a nitride powder with the desired properties. It has also been questioned whether this method really has the potential of yielding Si_3N_4 with low oxygen and carbon contents.

The overall reaction may be written as

$$3SiO_2(s) + 6C(s) + 2N_2(g) \rightarrow Si_3N_4(s) + 6CO(g) \quad (1)$$

If the quality demands could be met, carbothermal nitridation of silica should be a potential industrial process based on ubiquitous and cheap raw materials.

Various aspects of this process have been investigated during the last decades,[1-8] e.g. the dependence of conversion rates on temperature, starting material types and stoichiometry, homogenisation procedure and seeding. Within a current research programme we have studied reaction (1), starting with mixtures of C–SiO_2 and reacting them in nitrogen at *elevated pressures*.[9-12] This procedure expands the stability field of Si_3N_4 towards higher temperatures without concurrent SiC formation.[13] In the present work, the aim has been to gain information about the reactions that control the carbothermal reduction of quartz at different nitrogen pressures. Of particular interest were the chemical events during the primary period of a carbothermal nitridation run, when a typical C–SiO_2 mixture shows a high reactivity, vigorously evolving CO(g).

The reason for choosing quartz as a starting material was the possibility to check the amount of crystalline SiO_2 in the reacted samples by differential scanning calorimetry (DSC), in addition to the more frequently used methods: elemental analysis, X-ray diffraction and scanning electron microscopy (SEM). The morphology of quartz particles also makes it easy to distinguish between the quartz and carbon in the SEM and to identify the Si_3N_4 particles formed. As a coarse-grained powder was used, the evaporation rate from the SiO_2 surface in the reaction mixtures could be kept relatively low. This aided in controlling the SiO(g) generation, an important primary step in the carbothermal reaction.

2 Experimental

2.1 Materials

The starting materials were mixtures of quartz and carbon black powders, stoichiometric with respect to reaction (1) and pelletised to 'macaroni shaped' granules ($\phi \simeq 1{\cdot}5$ mm, $l = 3$–6 mm) after homogenisation with WC or SiAlON balls in an ethanol slurry. Two types of carbon powder (Nordisk Philblack Co., Malmö, Sweden), differing only in mean particle size; $\phi \simeq 20$ nm and $\simeq 70$ nm, were combined with two sieved fractions of quartz, $\phi < 100\,\mu m$ and $\phi < 34\,\mu m$, each from two different sources. The quartz from one source ('p.a.', E. Merck GmbH, Darmstadt, Germany) had been hand-ground in a mortar, and the other ('pure natural', provided by Gunnar Hällgren Kema Nord Industrikemi, Ljungaverk, Sweden) had been prepared in a planetary mill. For the machine-milled quartz fractions the total surface area was determined by the BET method and found to be $0{\cdot}28\,m^2/g$ ($\phi < 100\,\mu m$) and $1{\cdot}0\,m^2/g$ ($\phi < 34\,\mu m$). Due to the small amounts available no BET measurements could be made on the hand-ground material; but we believe, judging from SEM inspections and the different reactivities found, that it has a somewhat smaller total surface area than the corresponding machine-milled powder.

For the sake of brevity, the different reactants used will, in the following, be denoted as

C—carbon powder, $\phi \simeq 70$ nm, $A = 30\,m^2/g$ (BET)
c—carbon powder, $\phi \simeq 20$ nm, $A = 115\,m^2/g$ (BET)
Q—quartz powder, hand-ground, $\phi < 100\,\mu m$
q—quartz powder, hand-ground, $\phi < 34\,\mu m$
Q(0·3)—quartz powder, machine-milled, $\phi < 100\,\mu m$, $A = 0{\cdot}28\,m^2/g$ (BET)
q(1·0)—quartz powder, machine-milled, $\phi < 34\,\mu m$, $A = 1{\cdot}0\,m^2/g$ (BET)

In all experiments high-quality nitrogen ('Nitrogen PLUS', AGA Co., Lidingö, Sweden) was used without further purification.

2.2 Experimental set-ups

Two types of experimental set-up have been used, one for nitridation experiments at atmospheric pressure and the other for elevated pressures.

The experiments at atmospheric pressure were performed in a horizontal resistance furnace. The nitrogen gas flowing through an Al_2O_3 tube ($\simeq$1 litre/min) was preheated by letting it pass a perforated graphite plug in the hot zone before reaching the sample holder (Fig. 1). This was a horizontally placed graphite cylinder with a large vertical cavity for the sample and narrow horizontal channels to facilitate gas access. The sample holder, fixed at the end of a thermocouple, could quickly be moved from the cold to the hot zone inside the furnace. Nitridation runs, with holding times ranging from 15 min to 6 h, have been performed at 1450 and 1500°C. The thermocouple was calibrated, and the reading was found to be accurate to within ±10°C.

The nitridation experiments at elevated pressures were performed in a gas autoclave of 20 litres volume with a vertical graphite furnace. Runs were performed at different pressures (1–6 MPa), temperatures (1400–1680°C) and nitrogen gas flow rates through the sample holder (1·6–25 litres (STP)/min). During each run the amount of carbon monoxide (CO) formed was measured in the outlet gas by an IR-detector (Leco Corp., Svenska AB, Syndbyberg, Sweden) at room temperature and atmospheric pressure.

Our experience with the sample holder in the horizontal furnace proved this design to be too primitive (see below) for successful use with granulated charges of 0·1 g or larger. Therefore, a more elaborate and useful design was finally arrived at for the sample holder in the autoclave (Fig. 2). The basic idea is that all the reactant gas flowing through the furnace should pass the granulated sample, and then take the shortest way out of the furnace and pressure vessel to the CO-analyser. The charge was distributed in a granular mono-layer on a supporting perforated graphite foil (area $\simeq$ 7 cm^2) with approximately 50% coverage, and care was always taken to avoid uneven distribution or stacking of the granules. A standardised temperature programme, controlled by a PID regulator, was followed in all runs: rapid heating at a rate of 20°C/min to a constant temperature, holding at this plateau and then cooling at 30°C/min. The temperature was measured with a W–Re thermocouple, calibrated against the melting points of Au and Pd. The reading was found to be accurate to within ±5°C, while a constant temperature could be kept within ±1°C.

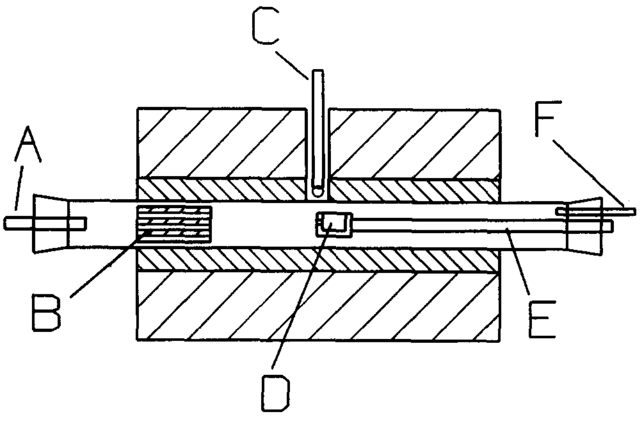

Fig. 1. Experimental set-up used for the atmospheric pressure experiments. (A) Gas inlet, (B) graphite plug for preheating the gas, (C) thermocouple for the furnace heat control, (D) sample holder, (E) thermocouple, and (F) gas outlet.

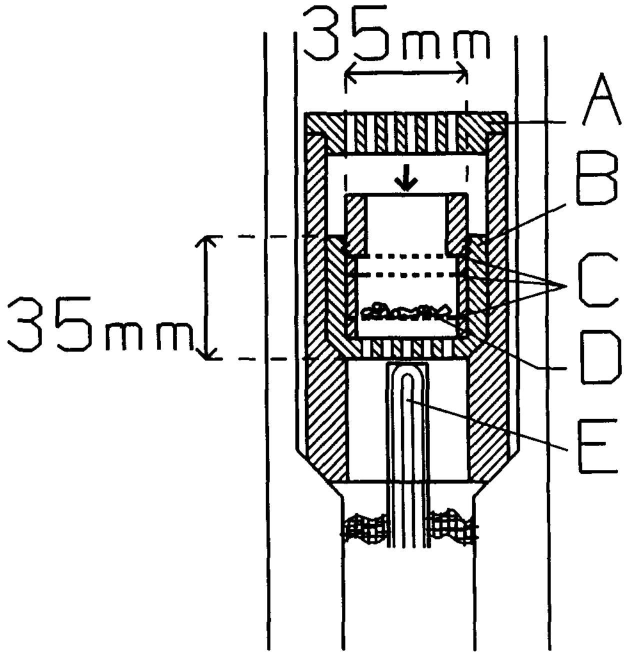

Fig. 2. Sample holder used in the autoclave at elevated pressures. (A) perforated lid, (B) sample holder with screw ring, (C) perforated graphite foils and spacer rings, (D) sample, and (E) Al_2O_3 and graphite thermocouple-shielding tubes.

2.3 Analyses

The degree of conversion of the starting materials was determined in different ways after each nitridation run. From elemental analyses (N, O, C) by means of fusion–extraction methods (performed by an independent laboratory), the amount of Si_3N_4 formed, as well as residual C and SiO_2, could be deduced. The relative weight change was also determined for the samples run at high pressures, confirming or not that the chemical reactions had

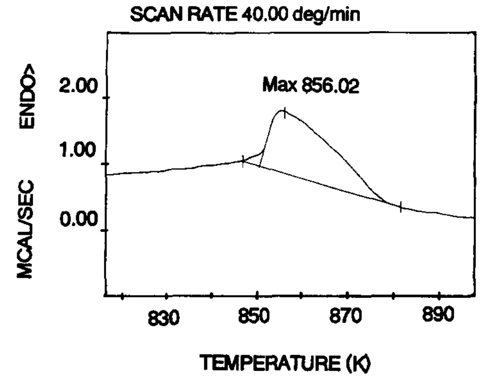

Fig. 3. Typical DSC curve of the quartz $\alpha \rightarrow \beta$ transformation in a quartz/carbon mixture.

actually proceeded according to the overall reaction (1). DSC was used as a fast and simple method to estimate the amount of crystalline SiO_2 (quartz or cristobalite) in the samples, taking advantage of the phase transitions $\alpha \rightarrow \beta$ in quartz at 573°C (Fig. 3) and $\alpha \rightarrow \beta$ in cristobalite, at 200–270°C.

The conversion of $\alpha \rightarrow \beta$ quartz is displacive and rapid, with a well investigated enthalpy of transformation,[14] but some factors may complicate the evaluation of the DSC peak area (which is proportional to $\Delta H(\alpha \rightarrow \beta)$). The difference in C_p between the two modifications of quartz gives rise to a shift of the base line from one side of the peak to the other, entailing some difficulty in defining the limits for the integral. Furthermore, the heat transfer between the sample and the thermocouple in the DSC-probe seems to be influenced to some extent by the carbon content. The heating rate used also affects the shape and resolution of the peak. This tends to decrease the accuracy of the measured ΔH value, unless an extensive calibration procedure is undertaken. Nevertheless, by using DSC (Perkin Elmer DSC-2) we have been able to make comparisons between the amounts of unreacted starting materials (quartz) and the residual SiO_2 in the samples. The accuracy was sufficiently good for valuable conclusions to be drawn about chemical events during the carbothermal synthesis (see below).

To identify crystalline phases, X-ray powder diffraction patterns recorded in focusing Guinier–Hägg cameras have been used. The relative proportions of the two Si_3N_4 modifications, α and β, were measured by means of a diffractometer, using the peak heights for a set of reflexions.[15] The reacted mixtures were checked in an SEM (JEOL 820 and 880) and analysed with an EDS micro-analysis system (LINK QX200 and AN10/85S). To reveal the inner morphology of the granule a cross-section was ultrasonically dispersed in ethanol and transferred to a substrate.

2.4 Thermodynamic calculations

Thermodynamic calculations were carried out on the system Si–O–N–C by use of the computer program SOLGASMIX[16] based on the principle of free energy minimisation. Our calculations were performed with 43 distinct gaseous and crystalline species. The data are, with one exception, taken from the JANAF tables.[17] The exception is Si_2ON_2(s), for which published thermodynamic data show a wide scatter. A review and a critical discussion have been given by Fegley.[18] In our calculations we have chosen the $\Delta G_f^0(Si_2ON_2)$-values that emerged in an equilibration study[19] based on chemicals, temperatures and pressures similar to those used in the present work.

It turned out in our calculations that *atomic* oxygen should be the dominant oxygen species at high temperatures and low oxygen partial pressures, while at low temperatures and higher oxygen partial pressure *molecular* oxygen dominates instead. In the following we will not discriminate between the two possibilities but use O(g), for the sake of simplicity. By $p_{(O)}$ in the text and diagrams we will mean the partial pressure sum of atomic and molecular oxygen.

3 Results and Discussion

3.1 Atmospheric pressure

In the experiments with nitrogen gas ($\Phi =$ 1 litre/min) flowing at atmospheric pressure, mixtures of Q and C were reacted for different times in the set-up shown in Fig. 1. It has the obvious advantage of being simple and permitting rapid heating and cooling of the charge.

By visual inspection we concluded that charges comprising more than just a few granules in no case became homogeneously reacted. In spite of our attempts to improve the gas access by extra venting channels in the graphite cylinder, the granules below the topmost layer were always found to be dark and partly unreacted. Even with a forced gas flow through the furnace tube, ensuring a high nitrogen concentration at the sample surface, mass transport of some gaseous species within the charge seemed to be rate-controlling for the nitridation process. Our subsequent work, as well as results published by others,[5–7,20] suggest that CO(g) is the crucial species.

Nevertheless, valuable information about the carbothermal nitridation process was obtained with this set-up. The results from the runs at 1500°C are presented in Figs 4–6. As the sample holder yielded an inhomogeneously reacted sample, all the product

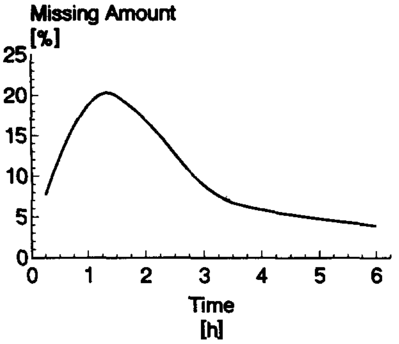

Fig. 4. The 'missing amount' in the atmospheric experiments at 1500°C, calculated from elemental analyses.

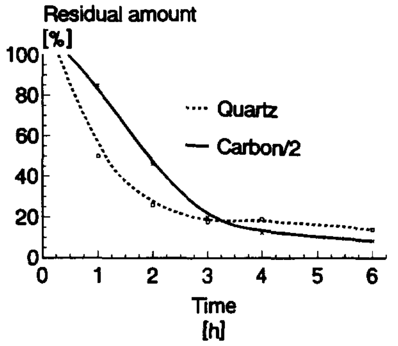

Fig. 5. Residual amounts of C and SiO_2 in the atmospheric experiments at 1500°C, calculated from elemental analyses.

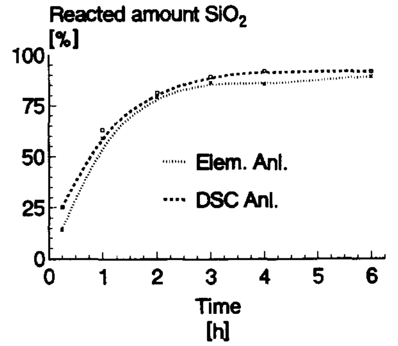

Fig. 6. Comparison of the reacted amount of SiO_2 in the atmospheric experiments at 1500°C, calculated from DSC and from elemental analyses.

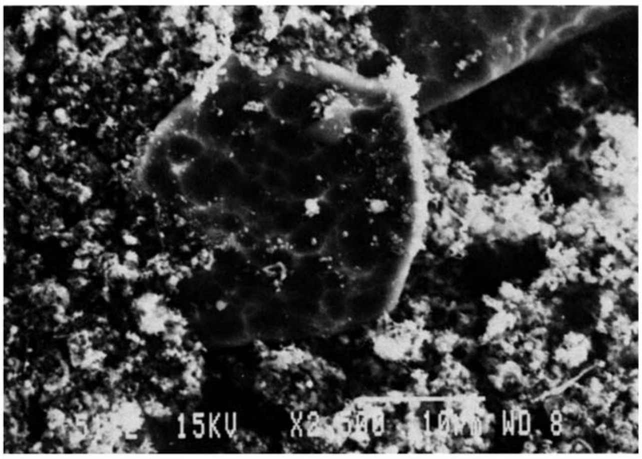

Fig. 7. SEM picture of a cross-section of a reacted granule from an experiment at atmospheric pressure, showing a clean quartz particle with pits all over the surface.

granules from a run were ground together prior to the analysis, so as to yield mean values.

SEM pictures of a cross-section of a reacted granule (Fig. 7) show how the quartz particles have reacted: pits have formed all over the surfaces, which are otherwise clean. Comparison with the starting materials shows that the particle size has decreased. This is most likely due to SiO(g) evaporation, primarily according to

$$SiO_2(s) + C(s) \rightarrow SiO(g) + CO(g) \quad (2)$$

$$SiO_2(s) + CO(g) \rightarrow SiO(g) + CO_2(g) \quad (3)$$

$$CO_2(g) + C(s) \rightarrow 2CO(g) \quad (4)$$

EDS micro-analyses showed that in an unreacted starting mixture only the quartz particles gave an Si signal, while in the reacted samples Si signals were also obtained from the carbon particles, indicating the direction of net Si transport on the microscopic level. In samples that were reacted to near completion, Si_3N_4 crystals could be identified as elongated hexagonal prisms and whiskers. These morphologies have commonly been reported for carbothermally produced Si_3N_4 crystals (see, for example, Refs 2 and 4). In the samples reacted for a shorter time, no particle that had a distinct morphology different from that of quartz could be found, except the few whiskers at the top of the charge.

Some of the reactions proposed in the literature, leading to Si_3N_4, are

$$3SiO(g) + 2N_2(g) + 3C(s) \rightarrow Si_3N_4(s) + 3CO(g) \quad (5)$$

$$3SiO(g) + 2N_2(g) + 3CO(g) \rightarrow Si_3N_4(s) + 3CO_2(g) (6)$$

followed by (4)

$$3SiO(g) + 2N_2(g) \rightarrow Si_3N_4(s) + 3O(g) \quad (7)$$

$$O(g) + C(s) \rightarrow CO(g) \quad (8)$$

$$O(g) + CO(g) \rightarrow CO_2(g) \quad (9)$$

followed by (4)

Which one of these that is really the final step in carbothermal nitridation has been a matter of controversy. In most publications the choice seems to be between (5) and (6). Reaction (7) followed by (8) has been suggested by Rahman and Riley.[5] The idea that nucleation starts as (5) but growth proceeds according to (6) has been put forward by Zhang and Cannon.[4,21] Our SEM observations show that the initial Si_3N_4-formation occurs preferentially close to the carbon surface, but we can not discriminate between (5), (6) or (7).

The known solid phases containing silicon that could form in the Si–C–O–N system are SiO_2, Si_2ON_2, Si_3N_4 and SiC. Assuming that the overall reaction proceeds according to (1), one can calculate the amount of C, SiO_2 and Si_3N_4 in a sample from the elemental analyses (C, O, N). If the assumption made is correct, the sum of formed Si_3N_4, and remaining C and SiO_2 should give a total of 100%, within the accuracy of the analysis. As a rule, the actual sums fell short of 100%, introducing a 'missing amount', plotted in Fig. 4. It can be seen that the discrepancy is smaller the longer the annealing period. From the analyses it is not possible to check if Si_2ON_2 has formed, since it can be written as a combination of SiO_2 and Si_3N_4:

$$SiO_2 + Si_3N_4 \rightarrow 2Si_2ON_2$$

However, no trace of Si_2ON_2 was seen in the X-ray powder patterns. If some of the silicon is bound in silicon carbide instead of silicon nitride, the sum of remaining C, SiO_2 and formed Si_3N_4 would be less than expected, and this could explain the missing amount observed. The strongest reflexions belonging to β-SiC, although diffuse, were actually observed in the powder photographs of the samples with high missing amounts. The silicon carbide formed, by some reaction parallel to reaction (1), will at a later stage in the synthesis react with nitrogen to form silicon nitride which should be thermodynamically stable under the pressure and temperature conditions in our experiments. This could possibly occur due to SiO(g)-generating reactions between SiC and SiO_2, as proposed by Lee and Cutler,[3] followed by one or more of the reactions (5), (6) or (7). The missing amount, that seems to be due to side reactions in the initial stage, will hence decrease with conversion of the starting mixture, which is the trend actually observed in the series of atmospheric pressure runs. The analytical discrepancy, the missing amount, could also be due to the formation of some micro-crystalline or amorphous oxycarbide. The existence of such phases have been reported in the literature.[22]

In this study the carbon:quartz molar ratio was 2:1 in the starting mixtures, i.e. it was stoichiometric according to reaction (1). After the atmospheric pressure runs, in particular those with short annealing times, we always found a carbon excess, obviously due to a net SiO(g) loss (Fig. 5). After longer reaction times, however, an oxygen excess was noted. This could be explained by the reoxidation of formed silicon nitride by impurity oxygen in the nitrogen gas, a process that is accelerated when little or no elemental carbon remains. In the comparison between the quartz conversion calculated from DSC and from elemental oxygen analyses, we found a good agreement (Fig. 6). All residual oxygen seems to be associated with the quartz; the SiO_2 starting material continuously transforms to a nitride or carbide phase, not temporarily to some other SiO_2 modification or amorphous SiO_2.

3.2 Elevated pressure

These experiments at atmospheric pressure clearly showed that for a comparison study of conversion rates and compositional changes in a dynamic nitrogen atmosphere, efficient venting of the gaseous reaction products must be provided for.

The importance of maximum gas access to all individual granules was further demonstrated in the development work on a sample holder for the high-pressure experiments. The design finally arrived at comprised a graphite crucible with perforated bottom, and graphite rings and foils, clamped together by a threaded ring, as shown in Fig. 2. Samples consisting of heaps of granules became inhomogeneously reacted, though, even with this arrangement. Figure 8 shows a cross-section through such a reacted heap of granules, a porous cake held together loosely by a 'fur' of Si_3N_4-whiskers. Nitridation had not gone to completion in this case, and a reaction zone can clearly be seen, that separates the light-grey nitridised parts, next to the free space above the charge and along the crucible walls and supporting foil, from the unreacted dark-grey centre of the 'heap'. Evidently, the fresh nitrogen gas flowing downwards in the sample container did not scavenge the interior of the charge efficiently from gaseous reaction products. Instead, the major gas stream seems to have passed along the

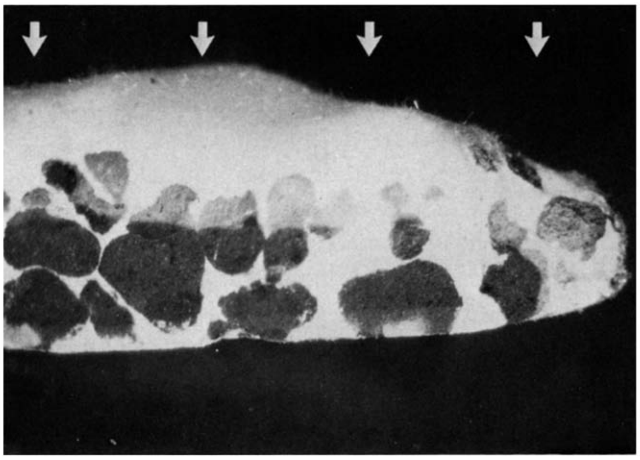

Fig. 8. Cross-section of a 'heap' of granules from a run at elevated pressure, showing a light-grey reacted zone separated from the dark unreacted centre of the 'heap'. N_2 flow direction indicated with arrows.

walls of the container and through the perforated foil.

That the adverse effect on nitridation is really caused by accumulated gaseous *products* was demonstrated by an experiment with three granular mono-layers of C–SiO_2 mixtures charged in the crucible, each on a supporting foil separated by a graphite ring. After a run, not long enough for complete reaction, all three layers were found to be homogeneously reacted, but while the Si_3N_4 conversion had proceeded far in the top layer, the middle layer was less reacted and the lower just a little. This shows that the reactant nitrogen gas, introduced at the top of the crucible, after contact with the C–SiO_2 charge at the highest level contains some gas species that retards the carbothermal nitridation downstream. Subsequent experiments with small amounts of CO mixed with the N_2 (see numbers 7, 12 and 14 in Table 1) proved that this adverse species is most likely CO(g), as mentioned earlier. Consequently, we have performed all subsequent nitridation runs in the autoclave with the reactant mixture spread in a granular mono-layer on the supporting graphite foil, where the fresh gas should have free access to the surface of all granules. At reasonably high nitrogen flows through the furnace, the Si_3N_4 conversion was found to be independent of gas flow rate, which is indicative of a useful sample holder design for our purpose.

The results of a number of runs at different temperature and pressure values, with granulated mixtures of carbon and quartz from different sources, are presented in Table 1. The starting mixture type, temperature, holding time, pressure and gas flow rate are noted. The 'yield', i.e. the molar ratio of Si in Si_3N_4 formed to SiO_2 charged, has been calculated for each run. The amount of unreacted quartz, determined by means of DSC, and total residual SiO_2 content, calculated from elemental analyses, are also presented. The 'extra evaporation loss' is defined as

$$\frac{\Delta m_{\mathrm{obs}}/m_0 - \Delta m_{\mathrm{anal}}/m_0}{\Delta m_{\mathrm{obs}}/m_0}$$

where m_0 is the charge weight, Δm_{obs} the weight change during the synthesis and Δm_{anal} the weight change calculated from elemental analysis of nitrogen, assuming reaction (1).

Table 1. Nitridation runs at 1470, 1550, 1680 and 1400°C

No.	*Mixture type*	*Temperature* (°*C*)	*Holding time* (*h*)	*p* (*MPa*)	Φ [*litres*(*STP*) *min*]	$\frac{\alpha}{\alpha+\beta}$ (%)	*Yield* (%)	*Extra evaporation loss* (%)	$\frac{m_{\mathrm{SiO_2}}}{m_{\mathrm{sample}}}$ (*O-anal*) (%)	$\frac{m_{\mathit{quartz}}}{m_{\mathrm{sample}}}$ (*DSC*) (%)
1	$c+q$	1 470	2	1·3	24	87	54	5·0	42	42
2	$c+Q$	1 470	2	1·3	18	100	51	5·7	44	41
3	$C+Q$	1 470	2	1·3	21	66	43	6·3	49	45
4	$C+Q$	1 550	2	0·7	5·5	63	79	5·0	19	14
5	$C+Q$	1 550	2	1·3	25	62	83	3·1	17	9
6	$C+Q$	1 550	2	2·5	25	59	86	0·8	16	5
7	$C+Q$ $N_2+3\%$ CO	1 550	2	1·4	5·5	—	3	—	63	16
8	$C+q(1{\cdot}0)$	1 550	2	2·5	21	50	93	3·9	4	0
9	$C+q(1{\cdot}0)$	1 550	2	1·5	1·7	87	70	8·4	27	0
10	$c+q(1{\cdot}0)$	1 550	2	1·5	20	64	84	6·5	15	0
11	$c+q(1{\cdot}0)$	1 550	2	1·5	1·7	91	62	12·4	32	0
12	$C+q(1{\cdot}0)$ $N_2+0{\cdot}1\%$CO	1 550	2	1·5	1·6	94	67	9·3	30	0
13	$C+Q(0{\cdot}3)$	1 550	0	1·5	1·8	—	7	43·4	71	34
14	$C+Q(0{\cdot}3)$ $N_2+1\%$ CO	1 550	0	1·5	1·7	—	4	56·1	72	30
15	$C+Q(0{\cdot}3)$	1 550	0	6·0	1·9	—	4	52·9	71	42
16	$C+Q(0{\cdot}3)$	1 550	0	1·5	17	—	11	26·1	68	44
17	$C+q(1{\cdot}0)$	1 550	0	1·5	1·8	—	11	17·2	69	14
18	$c+q(1{\cdot}0)$	1 550	0	1·5	1·8	—	16	24·2	67	15
19	$c+Q(0{\cdot}3)$	1 550	0	1·5	1·7	—	12	26·7	69	26
20	$c+q(1{\cdot}0)$	1 680	1	1·5	4	92	89	10·0	3	0
21	$C+q(1{\cdot}0)$	1 680	1	1·5	4	90	92	6·5	3	0
22	$C+Q(0{\cdot}3)$	1 680	1	1·5	4	77	82	10·6	11	0
23	$c+Q(0{\cdot}3)$	1 680	1	1·5	4	92	81	11·2	13	0
24	$c+q(1{\cdot}0)$	1 680	0	1·5	1·7	—	59	15·3	36	0
25	$C+Q(0{\cdot}3)$	1 400	0	1·5	1·8	—	2	67·0	72	69

3.2.1 Transformation of quartz—formation of Si_3N_4

In spite of analytical efforts we have not found any other crystalline or amorphous phase in the product mixtures in addition to Si_3N_4 and residual C and SiO_2. The most stable SiO_2 modification under prevailing pressure and temperature conditions should be cristobalite. Runs with quartz of different grain sizes have demonstrated, however, that with $\phi < 0{\cdot}2$ mm no detectable cristobalite formation ever occurs in parallel with reaction (1). Most of the sample stoichiometries turned out to be analytically straightforward, without any missing amount or other such effects.

It was found in our experiments that a great deal of the quartz reactant has been transformed already when the plateau temperature is reached at 1550°C, and virtually all quartz is consumed during the heating-up to 1680°C. As only a minor part of the SiO_2 reagent is converted to Si_3N_4 by the time the temperature reached 1550°C, most of the SiO_2 must then be present in an amorphous state. SEM pictures of samples run at 1550°C (Fig. 9) show that the typical original quartz particles with sharp edges and corners are replaced by small spherical particles or larger ones with smooth edges and rounded corners. The possibility of accidentally introduced impurities that could form low-melting silicates, were checked by X-ray micro-analysis, but no impurities could be found at levels $>0{\cdot}1\%$. The possibility of having an amorphous oxynitride phase was checked by N-analysis with an ultra-thin-window X-ray micro-analysis system, but no nitrogen signal was obtained from the spherical particles.

The quartz consumption during a temperature cycle was found to start even below 1400°C on heating-up; according to DSC it was 4% in run No. 25. Our analysis data thus indicate that at temperatures above ~1400°C, continuous SiO(g) evaporation from the quartz surface is responsible for rapid conversion of this reactant, even when the rate of Si_3N_4 formation is low. At elevated pressure, depending on the prevailing conditions, the SiO(g) generated can either be used up in Si_3N_4 formation or transformed to amorphous SiO_2. A part of the SiO(g) will also be swept away by the nitrogen flow and irreversibly lost. This 'extra evaporation loss' can be calculated from the weight change and elemental analysis of nitrogen, as mentioned earlier. In support of the view that gas-phase routes are the most important in this context is also the fact that the degree of quartz transformation in short runs is proportional to the quartz surface area, all other parameters being equal (cf. Nos 18 and 19).

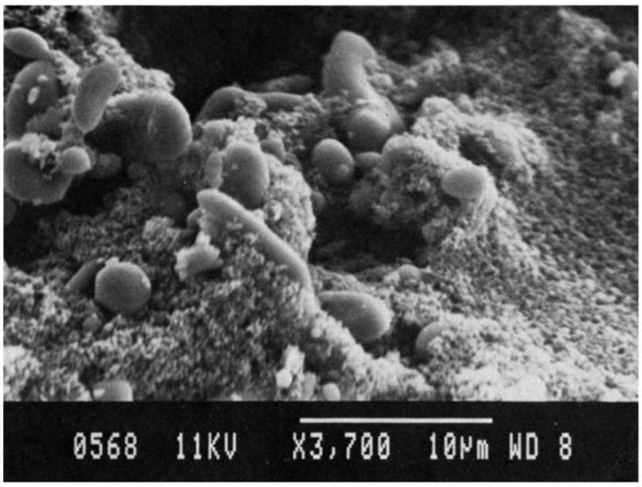

Fig. 9. SEM picture of a sample reacted at 1550°C and a pressure of 1·5 MPa for 1 min, showing spherical SiO_2 particles with smooth edges and corners in a carbon matrix.

3.2.2 The impetuous period

Incipient carbothermal nitridation of silica typically is accompanied by vivid CO(g) evolution, however followed by a fairly drastic decrease in reactivity on continued heating at constant temperature. This apparent 'impetuous period' with possible formation of non-equilibrium phases (SiC), as observed in our experiments at atmospheric pressure, is well-known to experimentalists[6,20] in the field. Some possible causes for the rapid decrease in reactivity are: decrease in surface area of the reactants, loss of contact between carbon and silica grains due to particle shrinkage, and build-up of produced nitride on reactant surfaces. Particularly with rapid heating to high temperatures and modest gas flows, the monitored CO signal displays a narrow peak at the beginning of the heat-treatment period. The maximum roughly coincides with the attainment of constant temperature, but it may occur before the plateau is reached. Figure 10 shows, as examples, the CO curves from runs 20–23, at 1680°C.

Conclusions can now be drawn about the chemical events during the first part of the annealing, causing the sudden loss of reactivity. To this end the short-time runs (Nos 13–19, 24, 25 in Table 1) are of particular interest. In these cases the heat-treatment did not extend beyond the impetuous period, and the rapid cooling (~30°C/min) should make estimations of the high-temperature phase relations possible.

The small amounts of N detected in samples heated up to the plateau temperature and then immediately quenched, correspond well to the total amount of CO evolved, assuming that all nitrogen is bound as Si_3N_4 formed according to reaction (1). In

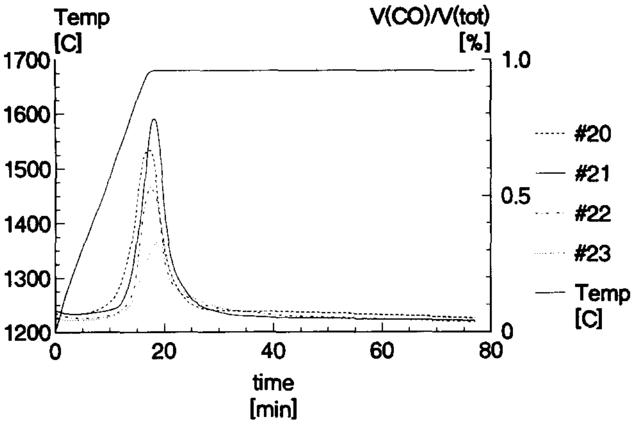

Fig. 10. CO curves for the four starting mixtures used. Temperature = 1680°C, pressure was 1·5 MPa.

run No. 18, for example, with starting mixture $c+q(1{\cdot}0)$ at 1550°C, 0·2 mmol of Si_3N_4 (16% yield) was produced, which would demand 1·2 mmol of CO(g) to be evolved. This is roughly the figure one obtains on integrating the CO curve. At this stage $\simeq 3$ mmol of quartz has been transformed, i.e. three-quarters of the original quartz content. After careful examination of SEM pictures we are convinced that no Si_3N_4 has been formed in the interior of the granules during such a short run to 1550°C. All nitrogen is therefore fixed in the Si_3N_4 whiskers growing on the granule surfaces.

It can be understood from thermodynamic considerations that nitride formation within the C—SiO_2 mixture does not begin until the end of the impetuous period. As has been discussed elsewhere,[11] restrictions set by $p_{(CO)}$ ($p_{(O)}$) on the Si_3N_4 precipitation in a C + SiO_2 mixture are rather severe, and the more so the higher the total pressure is, as demonstrated by the retarding effect of even small additions of CO to the N_2 gas in runs Nos 12 and 7. Generally, nitride formation will be hampered by a raise in $p_{(CO)}$, but favoured by a rise in $p_{(SiO)}$ (up to a certain limit). Table 2 shows the maximum CO and SiO contents of the N_2 atmosphere, as well as $p_{(O)}$, in equilibrium with C and Si_3N_4, calculated by means of the SOLGASMIX computer program for 1400°C, 1·0 and 3·0 MPa and 1700°C 1·5 MPa. The experimental temperatures are all within this range. The *real* $p_{(CO)}$ within the granules in our experiments at 1550°C is difficult to estimate, because of the dilution occurring in the sample holder, but it may well have exceeded the maximum for Si_3N_4-formation, in spite of the fairly low *measured* peak values of $v_{CO}/v_{tot} \simeq 0{\cdot}3\%$. This is why Si_3N_4 precipitation in the beginning of a run always exclusively took place on the outside of the granules, where $p_{(CO)}$ is a minimum due to the abundance of fresh nitrogen here. Consequently, we should not expect a retarding action due to nitride covering the reactants, at this stage. Formation of Si_3N_4 in the interior of the granules will start at the end of the impetuous period as soon as a sufficiently low $p_{(CO)}$ has been reached. This 'ignition point' depends on temperature and total pressure. The SEM and elemental analysis results indicated that, at 1550°C, no Si_3N_4 crystals formed within the pellet until the termination of the 'CO peak', while at 1680°C substantial nitridation had occurred already before the CO curve levelled out (cf. run No. 24 with almost 60% yield).

Table 2. Maximum calculated CO and SiO contents in the nitrogen coexisting with Si_3N_4 and C at 1400°C, 1·0 and 3·0 MPa and at 1700°C, 1·5 MPa

Temperature (°*C*)	p_{tot} (*MPa*)	$\frac{V_{co}}{V_{tot}}$ (%)	p_{SiO} (*Pa*)	p_O (*Pa*)
1400	1·0	1·4	8·3	$3{\cdot}8\times10^{-9}$
1400	3·0	0·7	5·7	$5{\cdot}5\times10^{-9}$
1700	1·5	5·8	610	$1{\cdot}4\times10^{-6}$

The SiO_2 transformation, on the other hand, is promoted by a high $p_{(CO)}$. This can be seen in Table 3, presenting values of $p_{(SiO)}$ and $p_{(O)}$ in equilibrium with solid SiO_2 at different v_{CO}/v_{tot} in N_2, all calculated by SOLGASMIX for 1400 and 1700°C, $p_{(tot)} = 1{\cdot}5$ MPa. For SiO(g) a self-generating process could thus in principle be operating in a rapidly heated C–SiO_2 mixture. Below 1400°C decomposition of SiO_2 starts producing SiO(g) and O(g). The latter reacts with C to give CO(g), acting on SiO_2 to accelerate the decomposition. The local $p_{(O)}$, a crucial parameter for the stability of both SiO_2 and Si_3N_4, is determined at every point within the powder mixture by the local rates of transport of the

Table 3. Equilibrium calculations with SOLGASMIX. N_2/CO gas mixtures in equilibrium with SiO_2 at 1400 and 1700°C, $p_{tot} = 1{\cdot}5$ MPa

Temperature (°*C*)	$\frac{V_{co}}{V_{tot}}$ (%)	p_{SiO} (*Pa*)	p_O (*Pa*)
1400	3·0	13·3	4.57×10^{-8}
1400	2·7	12·7	$4{\cdot}80\times10^{-8}$
1400	1·0	7·69	$7{\cdot}92\times10^{-8}$
1400	0·9	7·34	$8{\cdot}29\times10^{-8}$
1400	0·02	1·09	$5{\cdot}60\times10^{-7}$
1400	0·002	0·34	$1{\cdot}77\times10^{-6}$
1700	3·0	212	$2{\cdot}54\times10^{-4}$
1700	2·7	202	$2{\cdot}67\times10^{-4}$
1700	1·0	123	$4{\cdot}39\times10^{-4}$
1700	0·9	117	$4{\cdot}62\times10^{-4}$
1700	0·02	17·3	$3{\cdot}12\times10^{-3}$
1700	0·002	6·1	$8{\cdot}86\times10^{-3}$

main oxygen and silicon carriers (SiO(g), CO(g), CO_2(g), NO(g), according to the thermodynamic calculations). Of course, this assumption holds only if the pertinent chemical reactions are fast. The maximum values of $p_{(CO)}$ and $p_{(SiO)}$ reached are difficult to estimate as a steady flow of produced gaseous species will occur in the granules from the interior towards the surface. Due to the fairly high superficial flow rates of nitrogen and the relatively small granule size, a substantial drainage of CO(g), will limit $p_{CO,max}$ to maybe a few percent of $p_{(tot)}$.

The only mechanism we can suggest by which the condensation is brought about, is reduction of the local $p_{(CO)}$ at the SiO_2 surface, leaving the gas phase supersaturated with respect to SiO(g), which shifts the equilibrium back towards SiO_2(s).

$$SiO_2 + CO(g) \rightleftarrows SiO(g) + CO_2(g)$$

This is illustrated in the Table 3 for a 10% reduction of v_{CO}/v_{tot}, from 3·0 to 2·7% and 1·0 to 0·9%. A prerequisite for this mechanism to work is that CO(g) migrates faster than SiO(g) and CO_2(g) away from the saturated zone, which assumption is justified by the difference in molecular weights. The condensation must necessarily be adjacent to the quartz surface, judging from the narrow range of permissible $p_{(O)}$ (Table 3). We prefer to think that an 'evaporation–condensation zone' can move outwards from the centre of the granule, as the initially high $p_{(CO)}$ value in the interior is decreased by radial diffusion out to the surface of the granule. The SiO(g) reaching this surface, together with CO(g), reacts with the fresh N_2 to form Si_3N_4 whiskers. The maximum $p_{(CO)}$ within the zone occurs when the CO(g) generation balances the net CO(g) diffusion out of the zone. From this turning-point on, the SiO(g) generation decelerates as the SiO_2 surface area continuously decreases and $p_{(CO)}$ simultaneously starts to drop. The travelling zone will leave the originally fine-grained SiO_2 as coalesced particles, many with globular shape, as observed in the SEM (Fig. 9). The formation of zones has been observed and discussed in previous papers.[10,11] The relation between the CO evolution and the existence of a boundary separating a fully nitrided outer zone from a hard, sintered, poorly reacted core is, however, not yet completely known.

In conclusion we state that high-surface-area reactants may initially generate high CO(g)- and SiO(g)-contents in an intimate carbothermal mixture, resulting in high CO values in the sample holder. The coupled evaporation–condensation reactions sketched above will, however, rapidly reduce the SiO_2 surface area and so terminate the initial impetuous period of the carbothermal nitridation. CO(g) plays the role of actuator in this process, which is revealed by a fairly sharp peak in a continuously monitored CO signal from the sample space. In order to take advantage of the initially high reactivity of the carbothermal mixture and to optimise the yield of fine-grained Si_3N_4, one should use high temperatures, high nitrogen gas flows but moderately high pressures. If these conditions are not met, nitridation will primarily occur on the granule surfaces, giving a high whisker content in the nitride powder.

3.2.3 The dependence of reactivity on pressure, particle size and gas flow rate

The elemental and DSC analyses have revealed some interesting differences in reactivity among the different combinations of quartz; *Q*, *q*, *Q*(0·3) and *q*(1·0), and carbon; *C*, *c*, used as starting mixtures. It might be worthwhile trying to explain these differences within the framework of the model sketched above.

At the lowest temperature, 1470°C, a change in quartz particle size from *Q* to *q* in combination with *c*, and carbon from *C* to *c* in combination with *Q*, did increase the Si_3N_4 yield a little in 2 h runs at 1·3 MPa with similar gas flow rates (Nos 1–3). Evidently, the evaporation rate from even the larger-area quartz, *q*, was low enough not to exceed the rate of Si_3N_4 formation, as the residual SiO_2 was all (unreacted) quartz. Under these conditions—a relatively low temperature and an efficient nitrogen supply—it would pay to use more fine-grained starting materials to speed up nitridation to the limit set by carbon surface reactivity or gas-phase mass transfer.

In some previous studies[10,11] at 1410–1490°C on other C–SiO_2 mixture types comprising silica of higher surface area (50 m^2/g), we have found a larger variation in Si_3N_4 yield with C particle size. Systematic studies by others[4,8] using different C and SiO_2 qualities have shown that, in this temperature range, the Si_3N_4 conversion increased with increase in C surface area from 34 to 680 m^2/g, but was essentially independent of SiO_2 area in the range 50–380 m^2/g.

At 1550°C, 2 MPa, the more reactive starting mixtures comprising *q*(1·0) were almost completely nitridized after 2 h in high nitrogen flows (Nos 10 and 8), although still containing some residual amorphous SiO_2. Lower gas flow rates (1·7 litres (STP)/min) resulted in a lower yield, about the same for *C* and *c*, combined with *q*(1·0) (Nos 9 and 11). According to previous findings,[5,6,11] it is probably the more efficient removal of CO(g) from the granules that accomplishes the higher yield at a flow of 20 litres/min. A higher yield was reached with the finer quartz q(1·0) than with Q (Nos 8 and 6). The coarser carbon combined with q(1·0) was in fact found to give a higher yield, which is surprising. This may show that c transforms the SiO_2 more efficiently during the impetuous period, and so reduces the SiO_2 surface area more than C does.

As shown by the series Nos 4–6, conversion is somewhat increased by a pressure increase from 0·7 to 2·5 MPa and so is the quartz consumption. The decreased SiO_2 transformation at a still higher pressure, 6·0 MPa (No. 15), compared with 1·5 MPa (No. 13) might reflect the reduced mobility of gaseous species on a pressure increase.[12]

The slightly higher conversion reached in run No. 5, compared with No. 4, could also be due to the higher gas flow rate used in the former case. Based on our experience with this sample holder, however, and judging from the results of a number of previous carbothermal synthesis experiments,[12] we believe that with $\Phi(N_2) \geq 5$ litres/min the conversion is virtually independent of gas flow rate (i.e. of intergranular mass transfer in the charge).

One can notice a somewhat enhanced quartz consumption if a small amount of CO(g) is added to the nitrogen (No. 14, cf. No. 13). This suggests that the reactivity of the starting materials really is affected by small changes in $p_{(CO)}$ during the impetuous period, in support of the evaporation–condensation theory. The relatively low degree of quartz transformation found in the 'high-flow run' No. 16 (*cf.* No. 13), can then be explained by the decrease of $p_{(CO)}$ within the granules due to excessive CO(g) leakage to the surrounding atmosphere.

At the highest temperature, 1680°C, extensive nitridation had occurred even after a short run (No. 24). This is expected, due to the higher $p_{(CO)}$ threshold for Si_3N_4-formation at this high temperature (Table 2). Typical CO curves for four combinations of starting materials are shown in Fig. 10 (*cf.* Nos 20–23). By comparing the yields and the integrals of the CO peaks, it is clear that a change in quartz particle size from Q(0·3) to q(1·0) has a large impact on reactivity, while a change from C to c means less. We therefore conclude that with a SiO_2 surface area around 1 m^2/g and $\phi_c \simeq 70$ nm (BET carbon area = 30 m^2/g) the SiO gas evaporation is still rate-controlling for the nitridation process at 1680°C. The Si_3N_4 yield should benefit from an increased SiO_2 area, while a diminished carbon particle size has no effect. Of course, a final optimisation of the particle size must be done when gas flow rate and pellet size have been optimised.

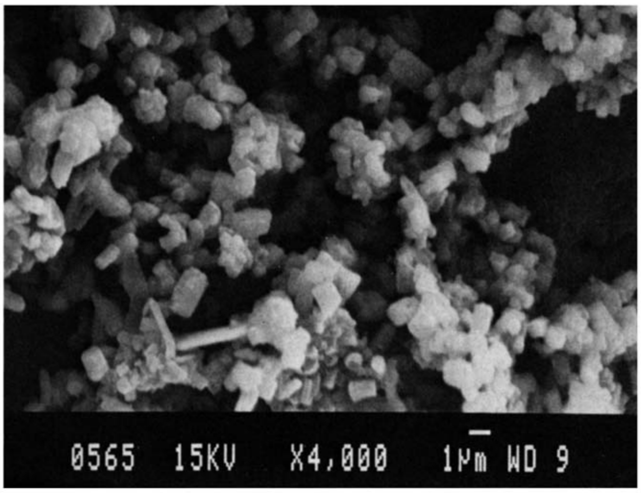

Fig. 11. SEM picture of a sample reacted at 1550°C at a pressure of 1·5 MPa for 2 h, showing formed Si_3N_4 particles.

3.2.4 The α/β-Si_3N_4 ratio

Even if the preparation time for the Si_3N_4 powder could be much reduced by a high gas flow rate, one should be aware that this also promotes formation of the β-modification. Our present data support the idea, presented and discussed elsewhere,[11] that in order to obtain powders with a high α-content, a high degree of supersaturation in the gas phase (from which α-Si_3N_4 precipitates) should be aimed at. Efficient drainage of SiO(g) and CO(g) from the granules by a high superficial gas flow has the opposite effect (e.g. Nos 8 and 10). On the other hand, reactive starting materials, a moderate total pressure and small additions of CO(g) to the process gas seem to promote the SiO(g) saturation with concomitant α-formation.

3.2.5 Particle morphology

The SEM pictures (Fig. 11) show that in the interior of the granules the Si_3N_4 crystals form short, approximately hexagonal prisms with relatively sharp corners and edges. This is the typical morphology also reported by other authors. The size of the 'boxes' varies from <0·5 μm up to 2–3 μm. The relation between the size of the particles and the process parameters is currently being investigated, and will be reported later.

4 Conclusions

(1) Comparative studies of conversion rates and phase relations in mixtures of C–SiO_2 at high temperatures in a dynamic nitrogen atmosphere demand a proper sample holder design, allowing sufficient flow rate and maximum access of the gas to all parts of the charge. Otherwise mass transport of

gaseous products within the sample space might easily be rate controlling for the overall nitridation process. CO(g) is such a product species that, on accumulation to even low levels within the reaction mixture, will hamper the formation of Si_3N_4.

(2) SEM and micro-analysis have shown that in carbothermal nitridation, at least at temperatures above 1400°C, the most important primary steps proceed via the gas phase. A steady flow from the SiO_2 surfaces feeds the gas with SiO(g) that may either take part in the Si_3N_4 precipitation or, depending on the conditions (temperature, $p_{(\mathrm{tot})}$, $p_{(\mathrm{CO})}$, $p_{(\mathrm{O})}, \ldots$), condense as amorphous SiO_2(s) or form SiC(s).

(3) At elevated pressure, typically most of the original SiO_2 content is transformed into amorphous condensed SiO_2 during the impetuous period characterised by an excessive CO(g)-evolution. This process is stimulated by the simultaneous CO formation. In the bulk of the reactant mixture, Si_3N_4 formation starts at the end of the impetuous period, when $p_{(\mathrm{CO})}$ ($p_{(\mathrm{O})}$) has reached sufficiently low levels. This $p_{(\mathrm{CO})}$ threshold is defined by temperature and $p_{(\mathrm{tot})}$.

(4) Si_3N_4 formation after the impetuous period will proceed at a rate determined by temperature and $p_{(\mathrm{CO})}$ ($p_{(\mathrm{O})}$), which is given by the rate of SiO(g) generation (SiO_2 surface area), the reducing capacity of the carbon (C carbon area) and the rate of CO transport out of the reaction zone.

(5) If a high yield of fine-grained Si_3N_4 is desired one should use a high temperature, a high gas flow rate through the sample but a moderately high pressure in the synthesis. If these conditions are not met, the formation of Si_3N_4 whiskers will be enhanced.

(6) It seems that formation of the α-modification of Si_3N_4 in the samples is favoured by a high degree of supersaturation of SiO(g) in the gas phase.

Acknowledgements

The authors wish to express their gratitude to Professor Lars Kihlborg for helpful discussions and valuable comments on the manuscript. Advice and help, mainly with analytical problems, from Gunnar Hällgren at Kema Nord Industrikemi, Ljungaverk is gratefully acknowledged, as is also the help of Dr Sven Westman at the Arrhenius Laboratory with correcting the English text. The contribution to part of the experimental work by Mr Pertti Hippinen is also appreciated. This work has received support from the Swedish Natural Science Research Council (NFR) and the Swedish Board for Technical Development (STU).

References

1. Hendry, A. & Jack, K. H., The preparation of silicon nitride from silica. In *Special Ceramics*, Vol. 6, ed. P. Popper. British Ceramic Research Association, Stoke-on-Trent, UK, 1975, p. 199.
2. Komeya, K. & Inoue, H., Synthesis of the alpha form of silicon nitride from silica. *J. Mater. Sci.*, **10**(7) (1975) 1243–6.
3. Lee, J. G. & Cutler, I. B., Reactions in the SiO_2–C–N_2 system. In *Nitrogen Ceramics*, ed. F. L. Riley. Noordhoff, Leyden, The Netherlands, 1977, p. 175.
4. Zhang, S.-C. & Cannon, W. R., Preparation of silicon nitride from silica. *J. Amer. Ceram. Soc.*, **67**(10) (1984) 691–5.
5. Rahman, I. A. & Riley, F. L., The control of morphology in silicon nitride powder from rice husk. *J. Europ. Ceram. Soc.*, **5** (1989) 11–22.
6. Figusch, V. & Ličko, T., Synthesis of silicon nitride powder by carbothermal nitriding of silica. In *High Tech. Ceramics*, ed. P. Vincenzini. Elsevier Publ. BV, Amsterdam, The Netherlands, 1987, p. 157.
7. Motoi, S. & Sasaki, S., Effects of N_2 and CO on the synthetic reaction of silicon nitride from silica. *Denki Kagaku*, **54**(2) (1986) 170–2.
8. Durham, S. J. P., Shanker, K. & Drew, R. A. L., Silicon nitride particle formation during carbothermal reduction. In *Ceramic Powder Processing Science*, ed. Hausner, Messing & Hirano, Proceedings of the Second International Conference, Berchtesgaden, FRG, 12–14 October 1988, p. 313.
9. Ekelund, M., Forslund, B., Niklewski, T., Eriksson, G., Hällgren, G., Johansson, T. & Hatcher, M., Establishment of the Si_3N_4/SiC phase boundary in the Si–C–O–N system at elevated pressures. In *Extended Abstracts*, Vol. 86(1), No. 392. The Electrochemical Society's 169th Meeting, 4–9 May 1986, Boston, MA, USA, 1986, p. 567.
10. Ekelund, M., Forslund, B. & Johansson, T., Study of the conversion of C + SiO_2 mixtures to Si_3N_4 in pressurized nitrogen. In *Ceramic Materials and Components for Engines*, ed. V. J. Tennery. The American Ceramic Society, Inc., USA, 1989, p. 101.
11. Ekelund, M. & Forslund, B., Carbothermal preparation of silicon nitride. Influence of starting material and synthesis parameters. *J. Amer. Ceram. Soc.*, in press.
12. Ekelund, M. & Forslund, B., Si_3N_4 Powder synthesis by high-pressure carbothermic nitridation of SiO_2: conversion as a function of gas flow rate and pressure. In *Ceramic Powder Science III*, ed. G. L. Messing. The American Ceramic Society, Inc., USA, 1990. p. 337.
13. Johansson, T., US Patent 4,530,825, 23 July 1985.
14. Majumdar, A. J., McKinstry, H. A. & Roy, R., Thermodynamic parameters for the α-β quartz and α-β cristobalite transitions. *J. Phys. Chem. Solids*, **25** (1964) 1487–9.
15. Käll, P. O., Quantitative phase analysis of Si_3N_4-based materials. *Chemica Scripta*, **28** (1988) 429–46.
16. Eriksson, G., Thermodynamic studies of high temperature equilibria. XII. SOLGASMIX, a computer program for calculation of equilibrium compositions in multiphase systems. *Chemica Scripta*, **8** (1975) 100–3.
17. *JANAF Thermochemical Tables* (2nd edn, NSRDS-NBS 37), ed. D. R. Stull & H. Prophet. National Bureau of Standards, Washington, DC, USA, 1971.
18. Fegley, M. B., The thermodynamic properties of silicon oxynitride. *J. Amer. Ceram. Soc.*, **64** (1981) C124.
19. Ekelund, M., Forslund, B., Eriksson, G. & Johansson, T.,

Si–C–O–N high-pressure equilibria and ΔG_f^0 for Si_2ON_2. *J. Amer. Ceram. Soc.*, **71**(11) (1988) 956–60.

20. Higgins, I. & Hendry, A., Production of β'-sialon by carbothermal reduction of kaolinite. *Brit. Ceram. Trans. J.*, **85** (1986) 161–6.
21. Cannon, W. R. & Zhang, S.-C., Nucleation and growth during carbothermal reduction and nitridization of silica. In *Ceramic Materials and Components for Engines*, ed. V. J. Tennery. The American Ceramic Society, Inc., Westerville, OH, USA, 1989, p. 86.
22. Julbe, A., Larbot, A., Guizard, C., Cot, L., Dupin, T., Charpin, J. & Bergez, P., Characterization of silicon oxycarbide species. *Europ. J. Solid State Inorg. Chem.*, **26** (1989) 101.